

1

2

3 Black Spot Gill Syndrome in the Northern Shrimp, *Pandalus borealis*, caused by the parasitic
4 ciliate *Synophrya* sp.

5

6

7 Richard F. Lee^{1*}, Anna N. Walker², Stephen C. Landers³, Tina L. Waters¹, Shirley A. Powell²,
8 Marc. E. Frischer¹

9

10

11 ¹ University of Georgia, Skidaway Institute of Oceanography, 10 Ocean Science Drive,
12 Savannah, Georgia 31411, USA

13 ² Mercer University School of Medicine, 1501 Mercer University Drive, Macon, Georgia 31207,
14 USA

15 ³ Department of Biological and Environmental Sciences, 210A MSCX, Troy University, Troy,
16 Alabama 36082, USA

17

18

19 *Corresponding Author

20 **ABSTRACT**

21 Black spot gill syndrome in the northern shrimp, *Pandalus borealis*, is caused by an apostome
22 ciliate, *Synophrya* sp., found within the gill lamellae. Whole mount staining, thin section
23 histology, electron microscopy, and molecular studies were carried out on infected gills. The
24 *Synophrya* 18S rRNA from *Pandalus borealis* (Genbank accession no. KX906568) and from
25 two portunid crab species, *Achelous spinimanus* (Genbank accession no. MH395150) and
26 *Achelous gibbesii* (Genbank accession no. MH395151) was sequenced. Phylogenetic analyses
27 confirmed the identity of these ciliates as apostomes. The 18S rRNA sequence recovered from
28 *P. borealis* shared 95% nucleotide similarity with the sequences recovered from the portunid
29 crab species suggesting that it is a different species of *Synophrya*. The invasive hypertrophont
30 stages, with a distinctive macronuclear reticulum, ranged in size from 300 to 400 μm with as
31 many as 5 large forms/ mm^2 of gill tissue. Histotrophic hypertrophont stages and hypertomont
32 stages were observed in these studies. The presence of the parasite was linked to the formation of
33 melanized nodules (up to 9 nodules/ mm^2 of gill tissue) by the host and in some cases to
34 extensive necrosis. Other studies have reported *Synophrya* sp. infections in *P. borealis* from
35 Greenland, Labrador and Newfoundland, but further studies are necessary to determine the
36 prevalence of this parasite in the dense schools of northern shrimp in the North Atlantic.
37 Questions remain as to the possibility of epizootics of this pathogen and its impact on northern
38 shrimp populations.

39

40 *Keywords:* *Synophrya*; *Pandalus borealis*; *black gill*; *necrosis*; *gill*; *northern shrimp*

41 **1. Introduction**

42 Crustaceans of commercial importance are infected by a variety of ciliated protozoan
43 parasites. Apostome ciliates are responsible for some widespread epidemics. For example, severe
44 outbreaks of darkened gill tissues, caused by a yet unidentified apostome ciliate and referred to
45 as black gill, have resulted in ongoing epidemics in *Litopenaeus setiferus* (white shrimp) and
46 *Farfantepenaeus aztecus* (brown shrimp) in the warm waters of the U.S. Southeast Atlantic
47 (Frischer et al., 2017). Black gill is hypothesized to be a contributing factor in the observed
48 decline of this fishery. Black spot gill syndrome in the commercially important pandalid shrimp,
49 *Pandalus borealis*, from cold high latitude waters has been shown to result from infection by an
50 unidentified ciliate (Apollonio and Dunstan, 1969; Rinaldo and Yevich, 1974). The goal of the
51 present work was to describe and identify the protist causing black spot gill syndrome in the
52 northern shrimp *Pandalus borealis* from coastal Maine.

53 Landings in Maine, USA of *P. borealis*, a shrimp species that often aggregates in dense
54 schools (Bergström, 2000; Garcia, 2007; Shumway et al., 1985), are highly variable. Up to 18
55 million pounds were harvested in 1996, but this peak was followed by a dramatic decline in
56 landings and moratoria have been instituted since 2014 (Atlantic States Marine Fisheries
57 Commission, 2015). In addition to the New England area of USA, there are important fisheries
58 for this shrimp in the Canadian Maritime Provinces, Greenland, Iceland, Norway, and Denmark.
59 Northern shrimp surveys carried out in the North Sea have shown very low population levels of
60 this shrimp since 2006 (Knutsen et al., 2015). Rinaldo and Yevich (1974) reported that 55% of *P.*
61 *borealis* collected in the Gulf of Maine from 1967 to 1970 had damaged, heavily melanized gills,
62 which they referred to as black spot gill syndrome. They suggested that this condition was
63 reducing commercial catches of *P. borealis*. Maine shrimp with this syndrome were first noted in

64 1966 and tentatively identified as caused by the ciliate *Gymnodinioides* sp. (Apollonio and
65 Dunstan, 1969). Rinaldo and Yevich (1974) could not confirm this identification but stated that
66 an unidentified protozoan was the causative agent of the syndrome. In this study we investigated
67 the identity of the black spot causing ciliate in *P. borealis* that remains present in epidemic
68 proportions in the Gulf of Maine, USA.

69

70 **2. Material and Methods**

71 *2.1 Collections*

72 Northern shrimp (*Pandalus borealis*) were collected from the Gulf of Maine in April 2016
73 (specific locations not available) and in March 2018 (43°46.5'N, 69°30.66'W). From each
74 collection, 10 shrimp representing a gradient of visible black spot syndrome symptoms (not
75 visible to very dark) were collected and stored on ice. Replicate gill tissue samples were
76 preserved within hours of collection in 70% non-denatured ethanol for PCR-based molecular
77 analysis, and in Zinc Formalin Fixative (Sigma Aldrich # Z2902) for histological examination.
78 For whole mount silver staining, thin section histology and electron microscopy, gill tissue was
79 fixed in either 4% cold glutaraldehyde in 0.2 µm filtered seawater or in 2.5% cold glutaraldehyde
80 buffered with 0.05M sodium cacodylate (pH 7.5). *P. borealis* collections were facilitated by the
81 Maine Department of Marine Resources. Portunid crabs including *Achelous gibbesii*, *Achelous*
82 *spinimamus* and *Achelous ordwayi* were collected (total of 48 crabs) during 3 cruises from the
83 mid-continental shelf at ca. 40 m depth at 31°21.3' N, 80°17.9' W in the South Atlantic Bight.
84 Collections were made on October 31, November 7 and December 5, 2017. Bottom trawls used a

85 12.2 m flat shrimp net with 4.8 cm stretch-mesh webbing throughout the body and bag. Tow
86 duration was 15 min of bottom time at a speed of approximately 2-3 knots.

87 *2.2 Whole mount analysis and staining*

88 Whole gills were examined with a stereomicroscope for melanized lesions caused by
89 *Synophrya*. Gill lamellae with the parasitic ciliates were separated, and stained with silver nitrate
90 using a modification of the Chatton-Lwoff silver impregnation technique (Chatton and Lwoff,
91 1935, Landers, 2008) to reveal the surface pattern of the parasite's ciliary rows.

92 *2.3 Routine Histology*

93 Zinc formalin-fixed gill tissues from *P. borealis* were processed for routine light microscopy
94 and embedded in paraffin. Sections (5 μm thick) were cut, mounted on glass slides, stained with
95 hematoxylin and eosin, coverslipped and examined using a light microscope. The ciliates and
96 nodules in 10 microscopic fields (400x) of each specimen were counted and reported as
97 numbers/ mm^2 of gill tissue.

98 *2.4 Thin section histology and electron microscopy*

99 Gill tissue fixed in cold glutaraldehyde was post-fixed in 2% osmium tetroxide. After post
100 fixation the samples were dehydrated and embedded in plastic for light microscopy histology and
101 transmission electron microscopy (TEM) (Landers, 2010) or were stored in 70 % ethanol for
102 scanning electron microscopy (SEM). Plastic sections for light microscopy (Spurr epoxy, EMS
103 Cat #14300) were cut at 1 micrometer thickness with a diamond knife on a Sorvall MT2B
104 ultramicrotome and stained with sodium borate-buffered toluidine blue for 10 seconds on a hot
105 plate. Tissue sections were observed using a light microscope. Tissues for SEM were dehydrated

106 to 100% ethanol, critical-point dried and sputter-coated with gold. The tissues were examined
107 using a Zeiss EVO 50 SEM at the Auburn University Research Instrumentation Facility
108 (AURIF) using both backscatter and secondary electron detectors. For TEM, -plastic-embedded
109 gill tissues were cut at 80-90 nanometers thickness and stained with uranyl acetate and lead
110 citrate. Sections were photographed using a Zeiss EM10 TEM at AURIF.

111 *2.5 Routine PCR and microscopy screening for Synophrya*

112 The presence of *Synophrya* in ethanol-preserved shrimp and crab gill tissue samples was
113 initially assessed using a previously described diagnostic PCR assay and the primer set Hyalo-
114 754F (5' GGA CAG TTG GGG GCA TTAGT) and Hyalo-952R (5' GAC CAA GTT ATA
115 AAA TGG CCA) (Frischer et al., 2017). This primer set amplifies an approximately 207 bp
116 fragment of the 18S rRNA gene from an apostome ciliate identified as *Synophrya* sp. detected in
117 *P. borealis* (Frischer et al., 2018). The presence of *Synophrya* sp. was confirmed in
118 representative crabs that screened positive for *Synophrya* sp. by microscopy.

119 *2.6 Cloning, sequencing and phylogenetic classification*

120 Nearly the complete small subunit rRNA (18S rRNA) gene of the ciliate associated with the
121 portunid crab was sequenced as previously described (Frischer et al. 2017). Prior to this study
122 the 18S rRNA gene of *Synophrya* from its originally described host (portunid crabs) had not
123 been sequenced. Total genomic DNA was purified from 70% ethanol-preserved gill tissue
124 collected from crabs that tested positive for *Synophrya* by PCR screening. DNA was purified
125 using the DNeasy® blood and tissue kit following the manufacturer's instructions (QIAGEN
126 inc., Valencia, CA, USA). The 18S rRNA gene was amplified utilizing the primers Hyalo-18SF-
127 754 and reverse Hyalo-18SR-952 paired with universal eukaryotic 18S rRNA primers, Univ-

128 18SF-15 (CTG CCA GTA GTC ATA TGC) and Univ-18SR-1765S (ACC TTG TTA CGA
129 CTT) (Gruebl et al. 2002). Cloning and sequencing was accomplished as previously described
130 (Frischer et al., 2017). Sequence alignments were facilitated using ClustalW (version 1.4) as
131 implemented in BioEdit software package using the default recommended weighting parameters
132 (Hall, 1999). Phylogenetic analysis was facilitated using the MEGA7 evolutionary analysis
133 software package (Kumar et al., 2016) after alignment of the recovered sequences with all
134 Apostomatia ciliate 18S rRNA sequences available from the Silva ribosomal database (SSU
135 r132) at the time of analysis. A total of 161 rRNA sequences from 8 Apostomatia divisions were
136 included. The majority of these sequences were not from identified specimens (127) and were
137 not represented by full-length sequences. To phylogenetically classify sequences from *P.*
138 *borealis* and the portunid crabs, an alignment of near full-length sequences (60) was assembled.
139 The 18S rRNA sequence from the hymenostome ciliate *Tetrahymena thermophila* (Genbank
140 accession no. M10932) was also included as an outgroup. Utilizing the available maximum
141 likely, neighbor joining, and maximum parsimony tree building algorithms implemented in the
142 MEGA7 software package, evolutionary reconstructions were inferred using the Maximum
143 Likelihood Tamura-Nei model (Tamura and Nei, 1993). Initial trees for the heuristic search were
144 obtained by applying the Neighbor-Joining method to a matrix of pairwise distances estimated
145 using the Maximum Composite Likelihood (MCL) approach. All positions containing gaps and
146 missing data were eliminated. There were a total of 1566 positions in the final dataset. All trees
147 were constructed with the appropriate bootstrap (100) procedures as implemented in MEGA7
148 (Kumar et al 2016).

149 **3. Results**

150 *3.1 Gross and light microscopic black spot gill syndrome pathology.*

151 The visible symptoms of black spot gill syndrome in *P. borealis* typically present as
152 macroscopic black spots in gill tissues, often with gross tissue necrosis apparent. These
153 symptoms are distinct and easily distinguished from general gill fouling (Fig. 1, 2A). In contrast,
154 the condition known as shrimp black gill, which is currently impacting penaeid shrimp
155 populations in the Southwest Atlantic and Gulf of Mexico, is caused by a different apostome
156 ciliate and presents as diffuse darkening of gill tissue (Gambill et al., 2015). During this study
157 the prevalences of black spot in *P. borealis* during both the 2016 and 2018 sampling were
158 estimated to be >80% (M. Hunter, personal communication).

159 Chatton-Lwoff silver nitrate impregnation (staining) of *Synophrya* confirmed the genus
160 identification and identified many characteristic life cycle stages known for *Synophrya* (Figure
161 2B-D). The hypertrophont stage was varied in its structure, which ranged from a simple sphere
162 (Fig. 2B) to oblong or multilobed. The hypertrophont has nine kineties (ciliary rows), which run
163 from pole to pole and are termed *meridional*. Additionally, positioned between kineties 9 and 1
164 are three kineties, x, y, and z. After bloating to many times its original size after invasion, likely
165 in response to chemical cues from the host's blood, the hypertrophont divides in order to release
166 small swimming stages into the host's cast off exoskeleton at molting (the dividing
167 hypertrophont stage is named the hypertomont). This divisional process is called
168 hyperpalintomy, during which there are successive divisions without intervening growth (Fig.
169 2C). The division of the hypertomont results in smaller cells with the same distinctive ciliature
170 as the previous stage. Eventually, the hypertomont daughter cells form the ultimate product of
171 hyperpalintomy, the hypertomites (Fig. 2D), which are released into the host's exuvium where
172 they begin the next feeding stage in the life cycle as they transform into exuviotrophic trophonts.
173 The ciliature and life cycle stages of the parasite from *P. borealis* is completely consistent with

174 the apostome ciliate genus *Synophrya*, known to infect crabs and shrimp along the United States
175 Atlantic and Gulf coasts (Johnson and Bradbury, 1976; Haefner and Spacher, 1985; Landers,
176 2010).

177 Examinations of microscopic sections of infected *P. borealis* gills revealed invasive
178 *Synophrya* that presented as large cytoplasmic masses (hypertrophonts) within the gill lamellae
179 and contained darkened cords of nuclear material (Fig. 3A-C). These cords were disconnected in
180 some sections as the structures wound into and out of the plane of section, and formed a distinct
181 macronuclear reticulum known to occur in this genus. These hypertrophonts were not observed
182 within the raphe of the gill, but only within individual lamellae, and were associated with distinct
183 melanization from the host reaction (Fig. 3B, C). The hypertrophont stages ranged in size from
184 300 to 400 μm (Fig. 3B-C) and were numerous, with as many as five large forms/ mm^2 (Fig. 3A,
185 Table 1). Additionally, later stages in the life cycle were observed, in which the hypertrophont
186 had divided (Fig. 3D). The small daughter cells, lacking the reticulate macronucleus, are the
187 hypertomites, which were also observed by whole mount silver staining (Figures 2D, 3D). In
188 some cases, small hypertomites (soon to develop into exuviotrophic trophonts) contained a
189 presumptive micronucleus visible within the cytoplasm next to the macronucleus (Figure 3D). In
190 addition to the feeding hypertrophont stages and the dividing stages, smaller ovoid cells attached
191 to the host's tissue were observed. These may have been settled phoront stages that had not
192 invaded the gill tissue to form hypertrophonts (Fig. 3C). These cells had a solid macronucleus
193 located within the central area of the cell.

194 The distribution of both large (hypertrophonts, Fig. 3A) and smaller forms (phoronts, Fig.
195 3C) was highly variable from specimen to specimen and also within the tissues of a given
196 specimen, ranging from non-detectable to 12 phoronts/ mm^2 (Table 1). The hypertrophonts

197 observed in the gill lamellae were associated with melanized nodules (Fig 3B, C, 4A, B), with up
198 to 9 nodules/mm² (Table 1). On occasion, necrosis of host tissues was observed and the parasite
199 was separated from adjacent host tissues by an accumulation of necrotic debris and melanin (Fig
200 3C). The hypertrophonts and divided stages were encapsulated by a cyst wall (Fig 3B, 4B).

201 3.2 *Electron microscopy*.

202 Scanning electron microscopy of infected gills revealed the bloated nature of individual
203 gill lamellae that contained *Synophrya* (Fig. 5A). No damage to the exoskeleton of the host was
204 visible, however. Transmission electron microscopy confirmed the presence of the *Synophrya*
205 cyst wall, which was approximately 2 μ m thick, homogeneous, and electron dense (Fig. 5B). The
206 cyst wall is known to be semi-permeable because nutrients from the host's tissue must cross this
207 structure to be absorbed by the mouthless parasite. The cyst wall from *Synophrya* in the Gulf of
208 Maine was indistinguishable from that of the *Synophrya* species in the Gulf of Mexico (Landers
209 2010).

210 3.3 *Phylogenetic Identification*

211 Nearly the complete 18S rRNA gene from the *Synophrya* infecting *P. borealis*, and from the
212 portunid crabs *A. spinimanus* and *A. gibbesii* collected from the South Atlantic Bight continental
213 shelf were sequenced. All sequences were deposited in Genbank (accession nos. KX906568,
214 MH395150, MH395151). The *Synophrya* sp. 18S rRNA sequences obtained in this study
215 clustered most closely with *Gymnodinioides* sp. JCC-2008 (Genbank accession no. EU503535)
216 and *Vampyrophrya pelagica* (Genbank accession no. EU503539) in a clade distinguished from a
217 clade consisting of representatives of the genera *Hyalophysa* and the ciliate that causes black gill
218 in penaeid shrimp (sBG ciliate, Genbank accession no. KX906567; bootstrap = 79%). The

219 similarity between the two *Synophrya* sp. strains associated with the portunid swimming crabs *A.*
220 *spinimanus* and *A. gibbesii* was high. Only a single nucleotide difference over the full gene was
221 observed indicating that the infecting ciliates in both crab species are almost certainly the same
222 species. Slightly greater differences were observed between the sequences recovered from the
223 portunid crabs and the shrimp *P. borealis*. Sequences were 95% similar with a total of 80
224 nucleotide differences over the entire gene (Figure 6). This level of difference is consistent with
225 at least a species level difference although it may indicate a higher order (genus) difference
226 (Clamp et. 2008).

227

228 **4. Discussion**

229 The cause of the black spot gill syndrome in the northern shrimp, *P. borealis*, is parasitization
230 by the apostome ciliate, *Synophrya* sp. The earliest studies on *Synophrya hypertrophica* were
231 carried out by Chatton and Lwoff (1926a, b; 1927; 1935) who described the structure and
232 complex life cycle of this this apostome ciliate in a number of crab species from the Brittany
233 coast and the Mediterranean coast of France. Later studies reported *Synophrya* sp. in portunid
234 crabs from the offshore waters of Spain and Tunisia (Sprague and Couch, 1971), in decapods
235 collected off the US South Atlantic (Johnson and Bradbury, 1976; Haefner and Spacher, 1985),
236 and in the swimming crab, *Portunus* (now *Achelous*) *spinicarpus*, from the Gulf of Mexico
237 (Landers, 2010). The ciliate seems to be restricted to high salinity offshore waters and is absent
238 in decapods from estuaries (Johnson and Bradbury, 1976). While most studies have reported on
239 *Synophrya* sp. in portunid crabs, the genus has also been reported parasitizing the brown rock
240 shrimp (*Sicyonia brevirostris*) and one specimen of the white shrimp (*Litopenaeus setiferus*)
241 (Johnson and Bradbury, 1976; Frischer, unpublished data). Annual surveys (2001 to 2009) of *P.*

242 *borealis* in waters off Labrador and Newfoundland reported the presence of black spot gill
243 syndrome in each year of the survey with parasite prevalence ranging from 1 to 13% (Orr et al.,
244 2011). Black spot gill syndrome in *P. borealis* from the Maine coast is highest (55%) in the
245 winter months (Rinaldo and Yevich, 1974) and thus the relatively low prevalence reported from
246 Labrador and Newfoundland may have differed due to collection in the fall (Orr et al., 2011).
247 Rinaldo and Yevich (1974) noted that *P. borealis* collected off Greenland were parasitized by
248 ciliates similar to those observed in northern shrimp from Maine waters Based on these
249 observations, we suggest that *Synophrya* is present in *P. borealis* from most North Atlantic
250 waters.

251 It remains unclear why black spot gill syndrome occurs at epidemic levels in the Gulf of
252 Maine. One factor may be related to relatively warmer temperatures in the Gulf of Maine
253 compared to more northern regions where northern shrimp currently support a major commercial
254 fishery. In the Gulf of Maine, *P. borealis* is at the southern extreme of its range and therefore
255 experiences subsurface water temperatures that are often above the 2 to 4 °C preferred by this
256 species (Shumway et al., 1985; Kavanaugh et al., 2017). Furthermore, in association with
257 climate change processes, water temperatures have been increasing in the Gulf of Maine at a
258 rapid rate, having increased at a rate of 0.1 to 0.4 °C per decade over the past 4 decades, faster
259 than most other oceanic regions (Kavanaugh et al., 2017; Poppick, 2018). This warming trend
260 may be associated with an increase in black spot gill syndrome and possibly other diseases.
261 Warming water temperatures have been associated with increased prevalence of disease in other
262 coastal invertebrate species. For example, on the east coast of the USA warming waters have
263 been linked to the spread of several oyster diseases caused by protist parasites (Harvell et al.,

264 1999; Ford, 1996). Although strictly speculation at this time, we suggest that if high latitude
265 waters continue to warm, black spot gill syndrome and could spread in *P. borealis* populations.

266 The life cycle of *Synophrya hypertrophica*, described by Chatton and Lwoff (1927, 1935)
267 and recently reexamined based on slides archived by Chatton (d'Avila et al. 2016), has two
268 phases, an invasive histotrophic phase and an exuviotrophic phase. The histotrophic phase is the
269 hypertrophont, which grows within the host's gill and is eventually stimulated to divide prior to
270 the molt of the host. The dividing stage is the hypertomont, that likely develops based on a
271 chemical cue from the pre-molt host. The related apostome *Hyalophysa chattoni*, while attached
272 to the shrimp's exoskeleton, is also known to metamorphose in response to the molting stage of
273 the host (Landers 1986). As the hypertomont divides, it produces hypertomite stages which are
274 released into the exoskeleton cast off by the host, where they mature further and feed on exuvial
275 fluid as trophonts. These exuviotrophic trophonts eventually encyst and divide to form
276 swimming stages that will attach to a host to begin again the invasive phase of the life cycle.
277 Thus, *Synophrya* sp. is unique, feeding both on tissue and on exuvial fluid during two different
278 phases of the life cycle. *Synophrya* sp. is also evidently related closely to the common
279 exuviotrophs, such as *Hyalophysa* and *Gymnodinioides* (Fig 6), and is morphologically
280 indistinguishable from *Gymnodinioides* in the exuviotrophic feeding stage (this feeding stage is
281 the basis for species identification in the apostomatida). *Synophrya* sp. can be easily diagnosed
282 by its large hypertrophont stages with the reticulated macronucleus, located within the gill tissue
283 of decapods. The reticulated macronucleus is a characteristic shared with other apostomes that
284 live in quite different hosts; for example, *Foettingeria* in the coelenteron of anemones,
285 *Chromidina* in kidneys of cephalopods, and *Pericaryon* in the lumen of ctenophores (Chatton
286 and Lwoff 1935). Further confirmation of the *Synophrya* genus is established by silver staining,

287 which reveals the characteristic ciliary rows (kinetics) 1–9 and xyz in the hypertrophont as well
288 as the divisional stages. However, identification of *Synophrya* to the species level is difficult. It
289 is tempting to assign the ciliate reported herein to the only known species, *S. hypertrophica*, as
290 our results are consistent with that identification. However, comparison of the 18S rRNA gene
291 sequences between the ciliates collected from portunid crabs and *P. borealis* suggest that the
292 *Synophrya* species found in *P. borealis* is a different species. Because different species may exist
293 that either have few morphological differences, or have differences in the life cycle that we have
294 not observed, the parasite from *P. borealis* is therefore identified at this time as *Synophrya* sp.

295 In the present study hypertrophonts and divisional stages were observed within gill tissues of
296 *P. borealis* and presumably were responsible for the pathologic changes. The observed dense
297 ring of melanin and focal necrosis are believed to be the result of the host immune effector cells
298 that attempt to surround, encapsulate and isolate the pathogen (Cerenius et al., 2010; Landers et
299 al., 2010). Additionally, it is interesting that the expanding hypertrophont stage absorbs its
300 nutrition from the host's blood across a cyst wall, which was observed by light microscopy and
301 transmission electron microscopy (TEM) in the current study. The TEM cyst wall data from the
302 current *Pandalus* study is consistent with the TEM images of *Synophrya* in the gills of the
303 portunid crab, *Achelous spinicarpus* (Landers, 2010).

304 The small attached ciliates observed in this study are consistent with apostome phoronts in
305 cell shape and nuclear shape. Given the *Synophrya* sp. hypertrophont infection, it is likely that
306 many of these cells are *Synophrya* phoronts that have not invaded the host's gill tissue. However,
307 as *Synophrya* is known to be sympatric with *Gymnodinioides* (Chatton and Lwoff, 1935) not all
308 of the attached phoronts can be assumed to be invasive.

309 **5. Conclusions**

310 Macroscopic black speckled spots in *P. borealis*, referred to as black spot gill syndrome, is
311 caused by the apostome ciliate, *Synophrya* sp. The invasive histotrophic forms, referred to as
312 hypertrophonts, are associated with heavy melanization and tissue necrosis, and are likely
313 responsible for observed pathologic changes. A different apostome ciliate is responsible for the
314 more diffuse black gill found in penaeid shrimp in the SE United States. We suggest that the
315 dense schools of *P. borealis* in the north Atlantic are susceptible to infection by the pathogenic
316 *Synophrya* sp. and because of the commercial importance of this shrimp stock, it is a priority to
317 monitor the spread and impact of black gill spot syndrome in northern shrimp populations. The
318 recent dramatic decreases in the northern shrimp catches in North Atlantic fisheries may be, in
319 part, due to the spread of black spot syndrome.

320 **Acknowledgments**

321 We thank Margaret Hunter from the Maine Department of Marine Resources who coordinated
322 the collection of northern shrimp samples and Katherine Thompson who sampled and preserved
323 gill tissues. Samples were collected by William Sherburne, Lessie White, Marilyn Lash and
324 Dana Hammond. Lee Ann DeLeo prepared the figures.

325 **Funding Sources**

326 This study was supported in part by an Institutional Grant (no. NA14OAR4170084) to the
327 Georgia Sea Grant College Program from the National Sea Grant Office, National Oceanic and
328 Atmospheric Administration and by an Institutional Grant (#NA16NOS4190165) to the Georgia
329 Department of Natural Resources from the Office from Coastal Management, National Oceanic
330 and Atmospheric Administration. Additional funding that allowed the collection of offshore
331 crabs was provided by the US National Science Foundation (to MEF) (OCE 1459239). The
332 statements, findings, conclusions, and recommendations are those of the authors and do not
333 necessarily reflect the views of the Georgia DNR, NOAA, or the NSF.

334 **References**

335 Apollonio, S., Dunstan, E.F., 1969. The northern shrimp, *Pandalus borealis*, in the Gulf of
336 Maine. Maine Department of Sea and Shore Fisheries, Report, Augusta, Maine, 81pp. (IP:S).

337

338 Atlantic States Marine Fisheries, 2015. Overview of stock status Northern Shrimp, *Pandalus*
339 *borealis*. http://www.asmfc.org/uploads/file//552ee6e0Northern_Shrimp_2015.pdf, accessed 6
340 December 2018.

341

342 Bergström, B.I., 2000. The biology of *Pandalus*. *Adv. Mar. Biol.*, 38, 55-245.

343

344 Cerenius, L., Soderhall, K., 2004. The prophenoloxidase-activating system in invertebrates.
345 *Immunol. Rev.* 198, 116-126.

346

347 Chatton, É., Lwoff, A., 1926a. Sur les parasites branchiaux internes du *Portunus depurator* et
348 sur leurs relations ontogénétiques probables avec les infusoires (Opalinopsidae) des céphalopods.
349 *C. R. Soc. Biol.* 94, 282-286.

350 Chatton, É., Lwoff, A., 1926b. Les *Synophrya* infusoires parasites internes des crabes. Leur
351 évolution à la mue. Leur place parmi les Foettingeriidae. *C. R. Ac. Sci. T.* 183, 1131-1134.

352 Chatton, É., Lwoff, A., 1927. Le cycle évolutif de la *Synophrya hypertrophica* (Cilié
353 Foettingeriidae). *C. R. Ac. Sci.* 185, 877-879.

354 Chatton, É. Lwoff, A., 1935. Les ciliés apostomes. 1. Aperçu historique et général: étude
355 monographique des genres et des espèces. *Arch. Zool. Exp. Gén.* 77, 1-453.

356 Clamp, J.C., Bradbury, P.C., Strüder-Kypke, M.C., Lynn, D.H., 2008. Phylogenetic position of
357 the apostome ciliates (Phylum Ciliophora, Subclass Apostomatia) tested using small subunit
358 rRNA gene sequences. *Denisia* 23, 395-402.

359 d'Avila-Levy, C. M., Yurchenko, V., Votypka, J., and Grellier P., 2016. Protist collections;
360 essential for future research. *Trends Parasitol.* 32, 840–842.

361 Ford, S.E., 1996. Range extension by the oyster parasite *Perkinsus marinus* into the northeastern
362 United States: response to climate change? *J. Shellfish Res.* 15, 45-55.

363 Frischer, M.E., Lee, R.F., Price, A.R., Walters, T.L., Bassette, M.A., Verdiyev, R., Torris, M.C.,
364 Bulaski, K., Geer, P.J., Powell, S.A., Walker, A.N., Landers, S.C., 2017. Causes, diagnostics, and
365 distribution of an ongoing penaeid shrimp black gill epidemic in the U.S. South Atlantic Bight. *J.*
366 *Shellfish Res.* 36, 487-500.

367 Frischer, M.E., Fowler, A.E., Brunson, J.F., Walker, A.N., Powell, S.A., Price, A.R., Bulski, K.,
368 Frede, R.I., Lee, R.F., 2018. Pathology, effects and transmission of black gill in commercial
369 penaeid shrimp from the South Atlantic Bight. *J. Shellfish Res.* 37, 149-158.

370 Gambill, J.M., Doyle, A.E., Lee, R.F., Geer, P.J., Walker, A.N., Parker, I.G., Frischer, M.E.,
371 2015. The mystery of black gill: shrimpers in the south Atlantic. Face off with a cryptic parasite.
372 *Current J. Mar. Educ.* 29, 2-7.

373 Garcia, E.G., 2007. The northern shrimp (*Pandalus borealis*) offshore fishery in the northeast
374 Atlantic. *Adv. Mar. Biol.* 52, 147-266.

375 Gruebl, T., Frischer, M.E., Sheppard, M., Neumann, M., Maurer, A.N., Lee, R.F., 2002.

376 Development of an 18S rRNA gene-targeted PCR-based diagnostic for the blue crab parasite

377 *Hematodinium* sp. Dis. Aquat. Org. 49, 61-70.

378 Haefner, P.A., Spacher, P.J., 1985. Gill meristics and branchial infestation of *Ovalipes*

379 *stephensoni* (Crustacea, Brachyura) by *Synophrya hypertrophica* (Ciliata, Apostomida). J. Crust.

380 Biol. 5, 273-280.

381 Hall, T.A., 1999. Bioedit: a user-friendly biological sequence alignment editor and analysis

382 program for windows 95/98/nt. Nucleic Acids Symp. Ser. 41, 95-98

383 Harvell, C.D., Kim, K., Burkholder, J.M., Colwell, R.R., Epstein, P.R., Grimes, D.J., Hofmann,

384 E.E., Lipp, E.K., Osterhaus, A.D.M.E., Overstreet, R.M., Porter, J.W., Smith, G.W., Vasta, G.R.,

385 1999. Emerging marine diseases-climate links and anthropogenic factors. Science 285, 1505-

386 1510.

387 Johnson, C.A., Bradbury, P.C., 1976. Observations on the occurrence of the parasitic ciliate

388 *Synophrya* in decapods in coastal waters off the southeastern United States. J. Protozool. 23,

389 252-256.

390 Kavanaugh, M.T., Rheuban, J.E., Luis, K.M.A., Doney, S.C., 2017. Thirty-three years of ocean

391 benthic warming along the U.S. northeast continental shelf and slope: patterns, drivers, and

392 ecological consequences. J. Geophys. Res. 122, 9399-9414.

393 Knutson, H., Jorde, P.E., Gonzales, E.B., Eigaard, O. R., Pereyra, R.T., Sannaes, H., Dahl, M.,

394 Andre, C, Søvik, G., 2015. Does population genetic structure support present management

395 regulations of the northern shrimp (*Pandalus borealis*) in Skagerrak and the North Sea. ICES J.
396 Mar. Sci. 72, 863-871.

397 Kumar, S., Stecher, G., Tamura, K., 2016. MEGA7: Molecular evolutionary genetics analysis
398 version 7.0 for bigger datasets. Mol. Biol. Evol. 33, 1870-1874.

399 Landers, S.C., 1986. Studies of the phoront of *Hyalophysa chattoni* (Ciliophora, Apostomatida)
400 encysted on grass shrimp. J. Protozool. 33, 546-552.

401 Landers, S.C., 2008. Staining improvements for apostome ciliates using a modified Chatton-
402 Lwoff technique. Southeastern Biology 55, 262.

403 Landers, S.C., 2010. The fine structure of the hypertrophont of the parasitic apostome *Synophrya*
404 (Ciliophora, Apostomatida). Eur. J. Protistol. 46, 171-179.

405 Orr, D., Veitch, P.J., Sullivan, D.J., Skanes, K., 2011. The status of the Northern shrimp
406 (*Pandalus borealis*) resource off Labrador and northeastern Newfoundland as of March 2010.
407 Fisheries and Oceans Canada, Canadian Science Advisory Secretariat. Research Document
408 2011/004, 175pp.

409 Poppick, L., 2018. Why is the Gulf Maine warming faster than 99% of the ocean? Eos 99
410 <https://doi.org/10.1029/2018EO109467>.

411 Rinaldo, R.G., Yevich, P., 1974. Black spot gill syndrome of the Northern shrimp *Pandalus*
412 *borealis*. J. Invert. Pathol. 24, 224-233.

413 Shumway, S.E., Perkins, H.C., Schick, D.F., Stickney, A.P., 1985. Synopsis of biological data on
414 the pink shrimp, *Pandalus borealis* Krøyer, 1938. NOAA Technical Report NMFS 30, U.S.
415 Department of Commerce, National Technical Information Service, Springfield, VA.

416 Sprague, V., Couch, J., 1971. An annotated list of protozoan parasites, hyperparasites and
417 commensals of decapod Crustacea. J. Protozool. 18, 526-537.

418 Tamura, K., Nei, M., 1993. Estimation of the number of nucleotide substitutions in the control
419 region of mitochondrial DNA in humans and chimpanzees. Mol. Biol. Evol. 10, 512-526.

420 **Figure Legends**

421 **Figure 1.** *Pandalus borealis* with black spot gill syndrome.

422 **Figure 2.** Light microscopy of unsectioned *Synophrya*. A. Low magnification image of *Pandalus*
423 *borealis* gills, with multiple *Synophrya* sp. parasites surrounded by the shrimp's melanin
424 reaction. B-D. Chatton-Lwoff silver nitrate staining. B. The hypertrophont stage. Kineties 1–9
425 and x, y, and z are visible as dark lines that run from pole to pole (meridional) on the enlarged
426 cell (arrows). C. The dividing hypertomont, with daughter cells revealing the characteristic
427 meridional kineties. D. Daughter cells from a hypertomont dissected from the gill, revealing
428 larger divisional stages as well as small hypertomite stages (arrow), characteristic of *Synophrya*
429 sp.

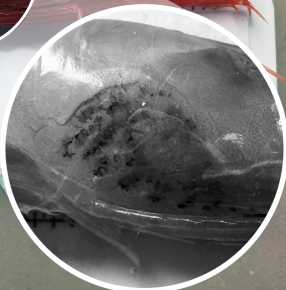
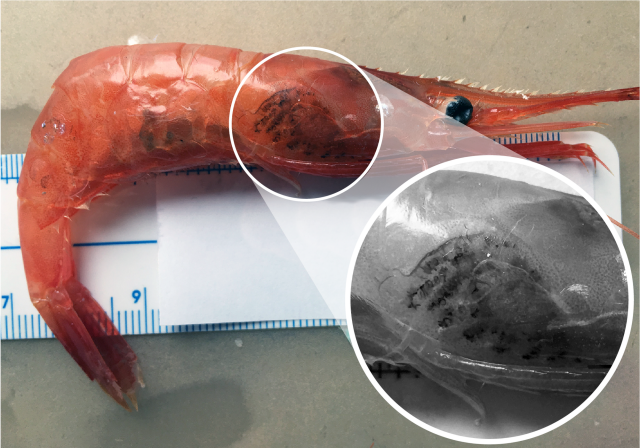
430 **Figure 3.** Paraffin sections of *Synophrya* sp. from *Pandalus borealis*. A. Overview of a gill
431 region with four parasites (arrows). B. A *Synophrya* sp. hypertrophont within a gill lamellum,
432 revealing the distinctive winding macronucleus within the cytoplasm. The host's melanization
433 reaction, used to isolate the parasite, is indicated (arrow) along with the cyst wall of the parasite
434 (arrowhead). C. A *Synophrya* sp. hypertrophont (star) revealing the complex macronucleus and
435 multiple lobes of this single cell. The host's melanization reaction is indicated (arrows). Non-
436 invasive apostome phoronts are indicated by arrowheads (Scale bar = 300 μ m). D. A *Synophrya*
437 sp. cyst wall filled with daughter cells following division. In two of the cells, a micronucleus is
438 visible (arrowheads).

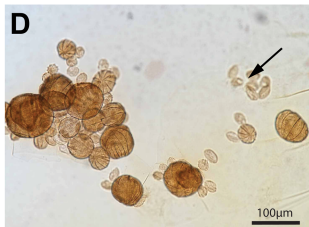
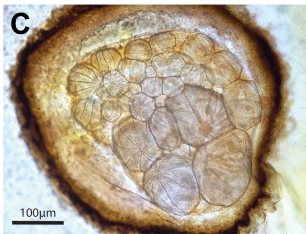
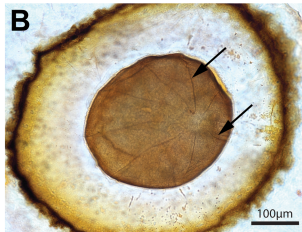
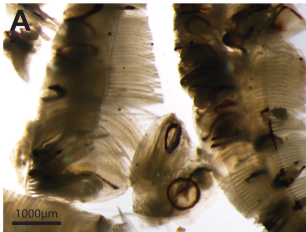
439 **Figure 4.** One- μ m thin sections of *Synophrya* sp. from *Pandalus borealis*. A. Two *Synophrya*
440 sp. parasites within the gill lamellae. The organism on the left is greatly enlarged and has caused
441 the lamellum to rupture. This cell may be in an early divisional stage, and thus, a hypertomont.
442 The host's melanization reaction typically encircles the parasite and is evident on either side of

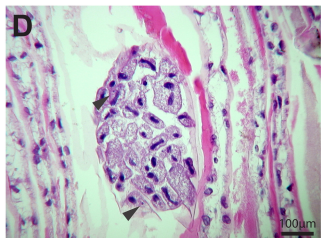
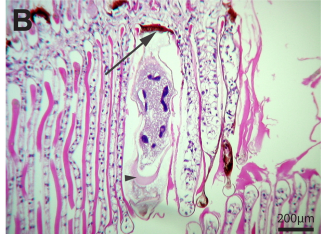
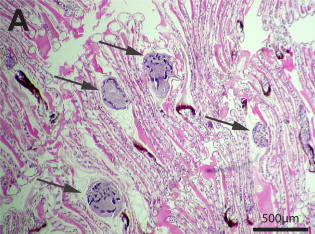
443 the smaller hypertrophont (arrows). B. Higher magnification reveals the semipermeable cyst
444 wall of the parasite (arrow) as well as the host exoskeleton (arrowhead). The melanization
445 reaction is visible on the right.

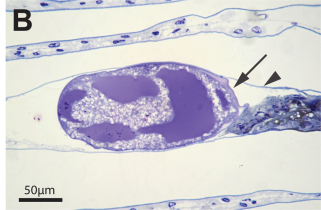
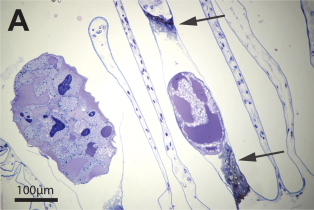
446 **Figure 5.** Electron microscopy of *Synophrya* sp. from *Pandalus borealis*. A. Scanning electron
447 microscopy of two enlarged lamellae (arrows) with *Synophrya* sp. parasites reveals little damage
448 to the outer exoskeleton. B. Transmission electron microscopy reveals the host's exoskeleton
449 (EX), the parasite cyst wall (CW), and the parasite cytoplasm (C) filled with lipid droplets (L).

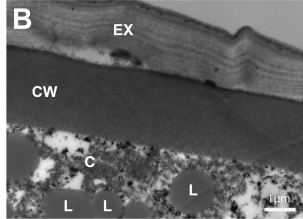
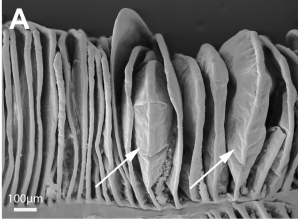
450 **Figure 6.** Inferred phylogenetic identity of *Synophrya* spp. Phylogenetic analysis was based on
451 the nearly complete 18S gene sequences from the *Synophrya* spp. associated with the Northern
452 shrimp *Pandalus borealis* (Genbank accession no. KX906568) and from the swimming crabs
453 *Achelous spinimanus* (Genbank accession no. MH395150) and *Achelous gibbesii* (Genbank
454 accession no. MH395151). Phylogenetic analyses were conducted in MEGA7 (Kumar et al
455 2016). The percentage of trees in which the associated taxa clustered together is shown next to
456 the branches (values < 75 are omitted). The tree is drawn to scale, with branch lengths measured
457 in the number of substitutions per site. The tree shown was constructed based on an alignment of
458 all available (60) near full length apostome ciliate rRNA sequences obtained from the Silva SSU
459 RNA database (SSU r132) although the portion of the tree shows only the *Synophrya* and
460 *Hyalophysa* clades. The hymenostome ciliate *Tetrahymena thermophila* (Genbank accession no.
461 M10932) was also included as an outgroup.

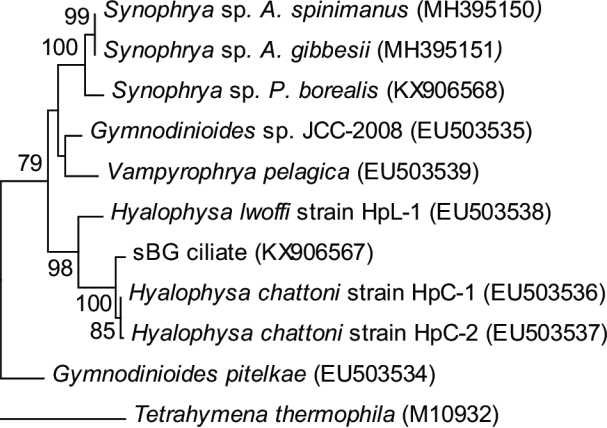












0.020

Table 1. Concentrations of black gill ciliates, hypertrophonts and hypertomonts, and nodules in *Pandalus borealis* gill tissues.

Sample Number	Ciliates/1mm ²	Hyper- forms/mm ²	Nodules/mm ²
1 (PB1)	7	0	1
2 (PB2)	5	0	0
3 (PB3)	12	0	0
4 (PB4)	3	1	1
5 (PB5)	6	0	1
6 (PB6)	1	2	9
7 (PB7)	3	5	6
8 (PB8)	1	0	6
9 (PB9)	4	0	1
10 (PB10)	0	4	4

